



**HAL**  
open science

## Wave Propagation in Porous Materials

Zine El Abiddine Fellah, Mohamed Fellah, Claude Depollier, Erick Ogam,  
Farid G. Mitri

► **To cite this version:**

Zine El Abiddine Fellah, Mohamed Fellah, Claude Depollier, Erick Ogam, Farid G. Mitri. Wave Propagation in Porous Materials. Computational and Experimental Studies of Acoustic Waves, 2018, 10.5772/intechopen.72215 . hal-01839659

**HAL Id: hal-01839659**

**<https://hal.science/hal-01839659>**

Submitted on 15 Jul 2018

**HAL** is a multi-disciplinary open access archive for the deposit and dissemination of scientific research documents, whether they are published or not. The documents may come from teaching and research institutions in France or abroad, or from public or private research centers.

L'archive ouverte pluridisciplinaire **HAL**, est destinée au dépôt et à la diffusion de documents scientifiques de niveau recherche, publiés ou non, émanant des établissements d'enseignement et de recherche français ou étrangers, des laboratoires publics ou privés.

---

# Wave Propagation in Porous Materials

---

Zine El Abiddine Fella, Mohamed Fella,  
Claude Depollier, Erick Ogam and Farid G. Mitri

Additional information is available at the end of the chapter

<http://dx.doi.org/10.5772/intechopen.72215>

---

## Abstract

This chapter provides different models for the acoustic wave propagation in porous materials having a rigid and an elastic frames. The direct problem of reflection and transmission of acoustic waves by a slab of porous material is studied. The inverse problem is solved using experimental reflected and transmitted signals. Both high- and low-frequency domains are studied. Different acoustic methods are proposed for measuring physical parameters describing the acoustic propagation as porosity, tortuosity, viscous and thermal characteristic length, and flow resistivity. Some advantages and perspectives of this method are discussed.

**Keywords:** acoustic porous materials, porosity, tortuosity, viscous and thermal characteristic lengths, fractional derivatives

---

## 1. Introduction

More than 50 years ago, Biot [1, 2] proposed a semi-phenomenological theory which provides a rigorous description of the propagation of acoustic waves in porous media saturated by a compressible viscous fluid. Due to its very general and rather fundamental character, it has been applied in various fields of acoustics such as geophysics, underwater acoustics, seismology, ultrasonic characterization of bones, etc. Biot's theory describes the motion of the solid and the fluid, as well as the coupling between the two phases. The loss of acoustic energy is due mainly to the viscosity of the fluid and the relative fluid-structure movement. The model predicts that the acoustic attenuation, as well as the speed of sound, depends on the frequency and elastic constants of the porous material, as well as porosity, tortuosity, permeability, etc. The theory predicts two compressional waves: a fast wave, where the fluid and solid move in phase, and a slow wave where fluid and solid move out of phase. Johnson et al. [3] introduced

---

the concept of tortuosity or dynamic permeability which has better described the viscous losses between fluid and structure in both high and low frequencies.

Air-saturated porous materials such as plastic foams or fibrous materials are widely used in passive control and noise reduction. These materials have interesting acoustic properties for sound absorption, and their use is quite common in the building trade and automotive and aeronautical fields. The determination of the physical parameters of the medium from reflected and transmitted experimental data is a classical inverse scattering problem.

Pulse propagation in porous media is usually modeled by synthesizing the signal via a Fourier transform of the continuous wave results. On the other hand, experimental measurements are usually carried out using pulses of finite bandwidth. Therefore, direct modeling in the time domain is highly desirable [4–10]. The temporal and frequency approaches are complementary for studying the propagation of acoustic signals. For transient signals, the temporal approach is the most

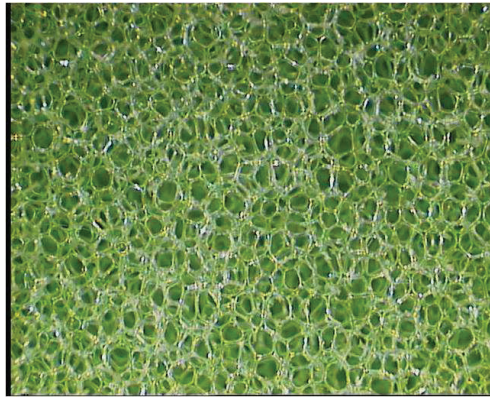


Figure 1. Air-saturated plastic foam.

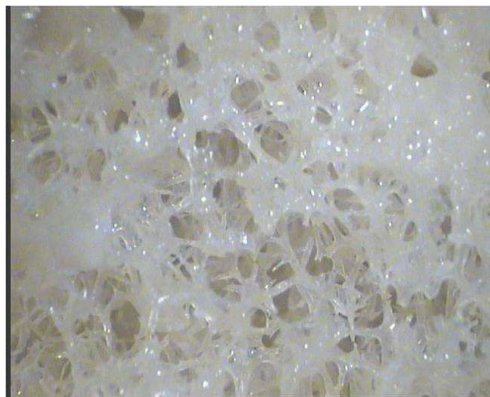


Figure 2. Human cancellous bone sample.

appropriate because it is closer to the experimental reality and the finite duration of the signal. However, for monochromatic harmonic signals, the frequency approach is the most suitable [11].

Fractional calculus has been used in the past by many authors as an empirical method to describe the viscoelastic properties of materials (e.g., see Caputo [12] and Bagley and Torvik [13]). The fact that acoustic attenuation, stiffness, and damping in porous materials are proportional to the fractional powers of frequency [4, 5, 7, 9, 10] suggests that fractional-order time derivatives could describe the propagation of acoustic waves in these materials.

In this chapter, acoustic wave propagation in porous media is studied in the high- and the low-frequency range. The direct and inverse scattering problems are solved for the mechanical characterization of the medium. The general Biot model applied to porous materials having elastic structure is treated, and also the equivalent fluid model, used for air-saturated porous materials (**Figures 1 and 2**).

## 2. Porous materials with elastic frame

In porous media, the equations of motion of the frame and fluid are given by the Euler equations applied to the Lagrangian density. Here,  $\mathbf{u}$  and  $\mathbf{U}$  are the displacements of the solid and fluid phases. The equations of motion are given by [1, 2]

$$\rho_{11} \frac{\partial^2 \mathbf{u}}{\partial t^2} + \rho_{12} \frac{\partial^2 \mathbf{U}}{\partial t^2} = P \nabla \cdot (\nabla \mathbf{u}) + Q \nabla (\nabla \cdot \mathbf{U}) - N \nabla \wedge (\nabla \wedge \mathbf{u}), \quad (1)$$

$$\rho_{12} \frac{\partial^2 \mathbf{u}}{\partial t^2} + \rho_{22} \frac{\partial^2 \mathbf{U}}{\partial t^2} = Q \nabla (\nabla \cdot \mathbf{u}) + R \nabla (\nabla \cdot \mathbf{U}), \quad (2)$$

where  $P$ ,  $Q$ , and  $R$  are the generalized elastic constants,  $\phi$  is the porosity,  $K_f$  is the bulk modulus of the pore fluid,  $K_s$  is the bulk modulus of the elastic solid, and  $K_b$  is the bulk modulus of the porous skeletal frame.  $N$  is the shear modulus of the composite as well as that of the skeletal frame. The equations which explicitly relate  $P$ ,  $Q$ , and  $R$  to  $\phi$ ,  $K_f$ ,  $K_s$ ,  $K_b$ , and  $N$  are given by

$$P = \frac{(1 - \phi) \left( 1 - \phi - \frac{K_b}{K_s} \right) K_s + \phi \frac{K_s}{K_f} K_b}{1 - \phi - \frac{K_b}{K_s} + \phi \frac{K_s}{K_f}} + \frac{4}{3} N, \quad Q = \frac{\left( 1 - \phi - \frac{K_b}{K_s} \right) \phi K_s}{1 - \phi - \frac{K_b}{K_s} + \phi \frac{K_s}{K_f}}, \quad R = \frac{\phi^2 K_s}{1 - \phi - \frac{K_b}{K_s} + \phi \frac{K_s}{K_f}}.$$

$\rho_{mn}$  is the “mass coefficients” which are related to the densities of solid ( $\rho_s$ ) and fluid ( $\rho_f$ ) phases by

$$\rho_{11} + \rho_{12} = (1 - \phi) \rho_s, \quad \rho_{12} + \rho_{22} = \phi \rho_f. \quad (3)$$

The Young modulus and the Poisson ratio of the solid  $E_s$  and  $\nu_s$  and of the skeletal frame  $E_b$  and  $\nu_b$  depend on the generalized elastic constant  $P$ ,  $Q$ , and  $R$  via the relations:

$$K_s = \frac{E_s}{3(1-2\nu_s)}, \quad K_b = \frac{E_b}{3(1-2\nu_b)}, \quad N = \frac{E_b}{2(1+\nu_b)}. \quad (4)$$

The mass coupling parameter  $\rho_{12}$  between the fluid and solid phases is always negative:

$$\rho_{12} = -\phi\rho_f(\alpha_\infty - 1), \quad (5)$$

where  $\alpha_\infty$  is the tortuosity of the medium. The damping of the acoustic wave in porous material is essentially due to the viscous exchanges between the fluid and the structure. To express the viscous losses, the dynamic tortuosity is introduced [3]  $\alpha(\omega)$  given by

$$\alpha(\omega) = \alpha_\infty \left( 1 - \frac{1}{jx} \sqrt{1 - \frac{M}{2} jx} \right) \quad \text{where} \quad x = \frac{\omega\alpha_\infty\rho_f}{\sigma\phi} \quad \text{and} \quad M = \frac{8k_0\alpha_\infty}{\phi\Lambda^2}. \quad (6)$$

where  $j^2 = -1$ ,  $\omega$  is the angular frequency,  $\sigma$  is the fluid resistivity,  $k_0$  is the viscous permeability, and  $\Lambda$  is the viscous characteristic length given by Johnson et al. [3]. The ratio of the sizes of the pores to the viscous skin depth thickness  $\delta = (2\eta/\omega\rho_0)^{1/2}$  gives an estimation of the parts of the fluid affected by the viscous exchanges. In this domain of the fluid, the velocity distribution is perturbed by the frictional forces at the interface between the viscous fluid and the motionless structure. At high frequencies, the viscous skin thickness is very thin near the radius of the pore  $r$ . The viscous exchanges are concentrated in a small volume near the surface of the frame  $\delta/r \ll 1$ . The expression of the dynamic tortuosity  $\alpha(\omega)$  is given by [3]

$$\alpha(\omega) = \alpha_\infty \left( 1 + \frac{2}{\Lambda} \left( \frac{\eta}{j\omega\rho_f} \right)^{1/2} \right), \quad (7)$$

The range of frequencies such that viscous skin thickness  $\delta = (2\eta/\omega\rho_0)^{1/2}$  is much larger than the radius of the pores  $r$

$$\frac{\delta}{r} \gg 1 \quad (8)$$

is called the low-frequency range. For these frequencies, the viscous forces are important everywhere in the fluid. When  $\omega \rightarrow 0$ , the expression of the dynamic tortuosity becomes

$$\alpha(\omega) \approx \alpha_0 \left( 1 + \frac{\eta\phi}{j\omega\alpha_0\rho_f k_0} \right), \quad (9)$$

$\alpha_0$  is the low-frequency approximation of the tortuosity introduced by Lafarge in [14] and Norris [15]:

$$\alpha_0 = \frac{\langle \mathbf{v}(\mathbf{r})^2 \rangle}{\langle \mathbf{v}(\mathbf{r}) \rangle^2} \quad (10)$$

where  $\mathbf{v}(\mathbf{r})$  is the microscopic velocity. The angle brackets represent the average of the random variable over the sample of material. In the time domain, and in the high-frequency domain, the dynamic tortuosity (Eq. 7)  $\alpha(\omega)$  acts as the operator, and its expression is given by [8]

$$\tilde{\alpha}(t) = \alpha_\infty \left( \delta(t) + \frac{2}{\Lambda} \left( \frac{\eta}{\pi \rho_f} \right)^{1/2} t^{-1/2} \right), \quad (11)$$

$\delta(t)$  is the Dirac function. In this model the time convolution of  $t^{-1/2}$  with a function is interpreted as a semi-derivative operator according to the definition of the fractional derivative of order  $\nu$  given by Samko et al. [16]:

$$D^\nu[x(t)] = \frac{1}{\Gamma(-\nu)} \int_0^t (t-u)^{-\nu-1} x(u) du, \quad (12)$$

where  $0 \leq \nu < 1$  and  $\Gamma(x)$  is the gamma function. A fractional derivative acts as a convolution integral operator and no longer represents the local variations of the function. The properties of fractional derivatives and fractional calculus are given by Samko et al. [16].

The introduction of the tortuosity operator  $\tilde{\alpha}(t)$  (Eq. 11) in Biot's Eqs. (1) and (2) to describe the inertial and viscous interactions between fluid and structure will express the propagation equations in the time domain. When  $\tilde{\alpha}(t)$  is used instead of  $\alpha_\infty$  in Eqs. (1) and (2), the equations of motion (1) and (2) will be written as [17]

$$\int_0^t \tilde{\rho}_{11}(t-t') \frac{\partial^2 \mathbf{u}(t')}{\partial t'^2} + \int_0^t \tilde{\rho}_{12}(t-t') \frac{\partial^2 \mathbf{u}(t')}{\partial t'^2} dt = P \cdot \nabla(\nabla \cdot \mathbf{u}(t)) + Q \nabla(\nabla \cdot \mathbf{u}(t)) - N \nabla \wedge (\nabla \wedge \mathbf{u}(t)),$$

$$\int_0^t \tilde{\rho}_{12}(t-t') \frac{\partial^2 \mathbf{u}(t')(t')}{\partial t'^2} + \int_0^t \tilde{\rho}_{22}(t-t') \frac{\partial^2 \mathbf{U}(t')}{\partial t'^2} dt = Q \nabla(\nabla \cdot \mathbf{u}(t)) + R \nabla(\nabla \cdot \mathbf{U}(t)). \quad (13)$$

In these equations, the temporal operators  $\tilde{\rho}_{11}(t)$ ,  $\tilde{\rho}_{12}(t)$ , and  $\tilde{\rho}_{22}(t)$  represent the mass coupling operators between the fluid and solid phases and are given by

$$\tilde{\rho}_{11}(t) = (1 - \phi) \rho_s + \phi \rho_f (\tilde{\alpha}(t) - 1), \quad \tilde{\rho}_{12}(t) = -\phi \rho_f (\tilde{\alpha}(t) - 1), \quad \tilde{\rho}_{22}(t) = \phi \rho_f \tilde{\alpha}(t),$$

where  $\tilde{\alpha}(t)$  is given by Eq. (11).

The wave equations of dilatational and rotational waves can be obtained using scalar and vector displacement potentials, respectively. Two scalar potentials for the frame and the fluid,  $\Phi_s$  and  $\Phi_f$ , are defined for compressional waves giving

$$\begin{pmatrix} \rho_{11} \frac{\partial^2}{\partial t^2} + A \frac{\partial^{3/2}}{\partial t^{3/2}} - P \Delta & \rho_{12} \frac{\partial^2}{\partial t^2} - A \frac{\partial^{3/2}}{\partial t^{3/2}} - Q \Delta \\ \rho_{12} \frac{\partial^2}{\partial t^2} - A \frac{\partial^{3/2}}{\partial t^{3/2}} - Q \Delta & \rho_{22} \frac{\partial^2}{\partial t^2} + A \frac{\partial^{3/2}}{\partial t^{3/2}} - R \Delta \end{pmatrix} \begin{pmatrix} \tilde{\Phi}_s(t) \\ \tilde{\Phi}_f(t) \end{pmatrix} = 0. \quad (14)$$

where  $A = \frac{2\phi\rho_f\alpha_\infty}{\Lambda} \sqrt{\frac{\eta}{\rho_f}}$ ,  $\Delta$  is the Laplacian, and  $\frac{\partial^{3/2}}{\partial t^{3/2}}$  represents the fractional derivative following the definition given by Eq. (12).

Two distinct longitudinal modes called fast and slow waves are obtained by the resolution of the eigenvalue problem of the matrix of Biot (Eq. (14)). On a basis of fast and slow waves  $\Phi_1(t)$  and  $\Phi_2(t)$ , one can have

$$\Delta \begin{pmatrix} \Phi_1(t) \\ \Phi_2(t) \end{pmatrix} = \begin{pmatrix} \tilde{\lambda}_1(t) & 0 \\ 0 & \tilde{\lambda}_2(t) \end{pmatrix} \begin{pmatrix} \Phi_1(t) \\ \Phi_2(t) \end{pmatrix}, \quad (15)$$

where  $\tilde{\lambda}_1(t)$  and  $\tilde{\lambda}_2(t)$  are the "eigenvalue operators" of the Biot matrix (Eq. (14)). Their expressions are given by

$$\tilde{\lambda}_i(t) = C_i \frac{\partial^2}{\partial t^2} + D_i \frac{\partial^{3/2}}{\partial t^{3/2}} + G_i \frac{\partial}{\partial t}, \quad i = 1, 2, \quad (16)$$

Their corresponding eigenvectors are

$$\tilde{\mathfrak{J}}_i(t) = A_i + \frac{B_i}{\sqrt{\pi t}}, \quad i = 1, 2, \quad (17)$$

where

$$C_i = \frac{1}{2} \left( \tau_1 + (-1)^i \sqrt{\tau_1^2 - 4\tau_3} \right), \quad D_i = \frac{1}{2} \left( \tau_2 + (-1)^i \frac{\tau_1\tau_2 - 2\tau_4}{\sqrt{\tau_1^2 - 4\tau_3}} \right),$$

$$G_i = (-1)^i \cdot \frac{1}{4} \left( \frac{\tau_2^2}{\sqrt{\tau_1^2 - 4\tau_3}} - \frac{(\tau_1\tau_2 - 2\tau_4)^2}{2(\tau_1^2 - 4\tau_3)^{3/2}} \right), \quad A_i = \frac{\tau_1 - 2\tau_5 + (-1)^i \sqrt{\tau_1^2 - 4\tau_3}}{2\tau_7},$$

$$B_i = \frac{1}{4\tau_7^2} \left[ \left( \tau_2 - 2\tau_6 + (-1)^i \frac{\tau_1\tau_2 - 2\tau_4}{\sqrt{\tau_1^2 - 4\tau_3}} \right) 2\tau_7 + \left( \tau_1 - 2\tau_5 - \sqrt{\tau_1^2 - 4\tau_3} \right) \cdot 2\tau_6 \right], \quad i = 1, 2,$$

and

$$\tau_1 = R'\rho_{11} + P'\rho_{22} - 2Q'\rho_{12}, \quad \tau_2 = A(P' + R' + 2Q'), \quad \tau_3 = (P'R' - Q'^2)(\rho_{11}\rho_{22} - \rho_{12}^2),$$

$${}^t\tau_4 = A(P'R' - Q'^2)(\rho_{11} + \rho_{22} - 2\rho_{12}), \quad \tau_5 = (R'\rho_{11} - Q'\rho_{12}), \quad \tau_6 = A(R' + Q'),$$

$$\tau_7 = (R'\rho_{12} - Q'\rho_{22}).$$

Coefficients  $R'$ ,  $P'$ , and  $Q'$  are given by

$$R' = \frac{R}{PR - Q^2}, \quad Q' = \frac{Q}{PR - Q^2}, \quad \text{and} \quad P' = \frac{P}{PR - Q^2}.$$

The fast and slow waves  $\Phi_1$  and  $\Phi_2$  are obeying to the following propagation equations along the  $x$  axis:

$$\frac{\partial^2 \Phi_i(x, t)}{\partial x^2} - \frac{1}{v_i^2} \frac{\partial^2 \Phi_i(x, t)}{\partial t^2} - h_i \frac{\partial^{3/2} \Phi_i(x, t)}{\partial t^{3/2}} - d \frac{\partial \Phi_i(x, t)}{\partial t} = 0, \quad i = 1, 2, \quad (18)$$

where the coefficients  $v_i, h_i (i = 1, 2)$ , and  $d$  are constants, respectively, given by

$$v_i = \frac{2}{\sqrt{\sqrt{\tau_1^2 - 4\tau_3} + (-1)^i \tau_1}}, \quad h_i = \frac{1}{2} \left( \tau_2 + (-1)^i \frac{\tau_1 \tau_2 - 2\tau_4}{\sqrt{\tau_1^2 - 4\tau_3}} \right), \quad i = 1, 2$$

and

$$d = -\frac{1}{4} \left( \frac{\tau_2^2}{\sqrt{\tau_1^2 - 4\tau_3}} - \frac{(\tau_1 \tau_2 - 2\tau_4)^2}{2(\tau_1^2 - 4\tau_3)^{3/2}} \right),$$

where Eq. (18) is a fractional propagation equations [17] in time domain of the fast and slow waves, respectively. These equations describe the attenuation and the spreading of the temporal signal propagating inside the porous material. These fractional propagation equations have been solved and well-studied in the case of rigid porous materials using the equivalent fluid model.

### 3. Porous materials with rigid frame

In the acoustics of porous media, two situations can be distinguished: elastic and rigid frame materials. In the first case, the Biot [1, 2] theory is best suited. In the second case, the acoustic wave cannot vibrate the structure. The equivalent fluid model is then used, in which the acoustic wave propagates inside the saturating fluid [8, 11]. The equations for the acoustics in the equivalent fluid model are given by

$$\rho \frac{\partial^2 U_i}{\partial t^2} = -\nabla_i p, \quad p = -K_f \nabla \cdot \mathbf{U}. \quad (19)$$

In these relations,  $p$  is the acoustic pressure. The first equation is the Euler equation, and the second one is a constitutive equation obtained from the equation of mass conservation associated with the behavior (or adiabatic) equation. These equations can be obtained from the Biot Eqs. (1, 2) by canceling the solid displacement. Assuming that the porous medium studied is homogeneous and has a linear elasticity, we obtain easily the following wave equation (propagation along the  $x$  axis) for the acoustic pressure in a lossless porous material:

$$\frac{\partial^2 p(x, t)}{\partial x^2} - \left( \frac{\rho}{K_a} \right) \frac{\partial^2 p(x, t)}{\partial t^2} = 0. \quad (20)$$

In Eq. (20), the viscous and thermal losses that contribute to the sound damping in acoustic materials are not described. The thermal exchanges are generally negligible near viscous effects in the porous materials obeying to the Biot theory, this is not the case for air-saturated

porous materials using the equivalent fluid model. To take into account the fluid-structure exchanges, the density and compressibility of the fluid are “renormalized” by the dynamic tortuosity  $\alpha(\omega)$  and the dynamic compressibility  $\beta(\omega)$ , via the relations  $\rho \rightarrow \rho\alpha(\omega)$  and  $K_f \rightarrow K_f/\beta(\omega)$ , giving the following wave equation in frequency domain (Helmholtz equation) for a lossy porous material:

$$\frac{\partial^2 p(x, t)}{\partial x^2} + \omega^2 \left( \frac{\rho\alpha(\omega)\beta(\omega)}{K_a} \right) p(x, t) = 0. \quad (21)$$

The thermal exchanges to the fluid compressions-dilatations are produced by the wave motion. The parts of the fluid affected by the thermal exchanges can be estimated by the ratio of a microscopic characteristic length of thermal skin depth thickness  $\delta' = (2\eta/\omega\rho P_r)^{1/2}$  ( $\eta$  is the fluid viscosity;  $P_r$  is the Prandtl number).

The expression of the dynamic compressibility is given by

$$\beta(\omega) = \gamma - (\gamma - 1) / \left[ 1 - \frac{1}{jx'} \sqrt{1 - \frac{M'}{2} jx'} \right] \quad \text{where } x' = \frac{\omega\rho_f k'_0 P_r}{\eta\phi} \quad \text{and } M' = \frac{8k'_0}{\phi\Lambda'^2}. \quad (22)$$

where  $\gamma$  is the adiabatic constant, the magnitude  $k'_0$  introduced by Lafarge [14] called thermal permeability by analogy to the viscous permeability, and  $\Lambda'$  is the thermal characteristic length. The low-frequency approximation of  $\beta(\omega)$  [14] is given by

$$\beta(\omega) = \gamma + \frac{(\gamma - 1)\rho_f k'_0 P_r}{\eta\phi j\omega}, \quad \text{when } \omega \rightarrow 0. \quad (23)$$

where  $k'_0$ , which has the same size (area) that of Darcy's permeability of  $k_0$ , is a parameter analogous to the parameter  $k_0$  but is adapted to the thermal problem.

In a high-frequency limit, Allard and Champoux [18] showed the following behavior of  $\beta(\omega)$ :

$$\beta(\omega) = 1 - \frac{2(\gamma - 1)}{\Lambda'} \left( \frac{\eta}{P_r \rho_f} \right)^{1/2} \left( \frac{1}{j\omega} \right)^{1/2}, \quad \omega \rightarrow \infty. \quad (24)$$

Replacing  $\alpha(\omega)$  and  $\beta(\omega)$  given by Eqs (18) in Eq. (21), we obtain the following lossy equation for porous materials in the high-frequency domain:

$$\frac{\partial^2 p(x, t)}{\partial x^2} + \omega^2 \frac{\rho\alpha}{K_a} \left( 1 - \sqrt{\frac{\eta}{\rho j\omega} \left[ \frac{2}{\Lambda} + \frac{2(\gamma - 1)}{\Lambda' \sqrt{\text{Pr}}} \right]} \right) p(x, t) + \left( \frac{D_1 - 1}{x} \right) \frac{\partial p(x, t)}{\partial x} = 0. \quad (25)$$

In the time domain (using the convention  $\partial/\partial t \rightarrow -j\omega$ ), we obtain the following fractional propagation equation:

$$\frac{\partial^2 p(x, t)}{\partial x^2} - \left(\frac{\rho\alpha}{K_a}\right) \frac{\partial^2 p(x, t)}{\partial t^2} - \frac{2\alpha\sqrt{\rho\eta}}{Ka} \left(\frac{2}{\Lambda} + \frac{2(\gamma - 1)}{\Lambda'\sqrt{Pr}}\right) \frac{\partial^{3/2} p(x, t)}{\partial t^{3/2}} = 0. \quad (26)$$

In this equation, the term  $\frac{\partial^{3/2} p(x, t)}{\partial t^{3/2}}$  is interpreted as a semi-derivative operator following the definition of the fractional derivative of order  $\nu$ , given by Samko and coll. [16]. The solution of the wave Eq. (26) with suitable initial and boundary conditions is by using the Laplace transform.  $F$  is the medium's Green function [9] given by

$$F(t, k) = \begin{cases} 0 & \text{if } 0 \leq t \leq k \\ \Xi(t) + \Delta \int_0^{t-k} h(t, \xi) d\xi & \text{if } t \geq k \end{cases} \quad (27)$$

with

$$\Xi(t) = \frac{b'}{4\sqrt{\pi}} \frac{k}{(t-k)^{3/2}} \exp\left(-\frac{b'^2 k^2}{16(t-k)}\right), \quad (28)$$

where  $h(\tau, \xi)$  has the following form:

$$h(\xi, \tau) = -\frac{1}{4\pi^{3/2}} \frac{1}{\sqrt{(\tau - \xi)^2 - k^2}} \frac{1}{\xi^{3/2}} \int_{-1}^1 \exp\left(-\frac{\chi(\mu, \tau, \xi)}{2}\right) (\chi(\mu, \tau, \xi) - 1) \frac{\mu d\mu}{\sqrt{1 - \mu^2}}, \quad (29)$$

$$\chi(\mu, \tau, \xi) = \left(\Delta\mu\sqrt{(\tau - \xi)^2 - k^2} + b'(\tau - \xi)\right)^2 / 8\xi, \quad b' = Bc_0^2\sqrt{\pi},$$

and  $\Delta = b'^2$ .

Let us consider a homogeneous porous material which occupies the region  $0 \leq x \leq L$ ; the expressions of the reflection and transmission coefficients in the frequency domain are given by

$$R(\omega) = \frac{(1 - D^2)\sinh(k(\omega)L)}{2Y(\omega)\coth(k(\omega)L) + (1 + Y^2(\omega))\sinh(k(\omega)L)}, \quad (30)$$

$$T(\omega) = \frac{2Y(\omega)}{2Y(\omega)\coth(k(\omega)L) + (1 + Y^2(\omega))\sinh(k(\omega)L)}, \quad (31)$$

where

$$Y(\omega) = \phi\sqrt{\frac{\beta(\omega)}{\alpha(\omega)}}, \quad \text{and} \quad k(\omega) = \omega\sqrt{\frac{\rho\alpha(\omega)\beta(\omega)}{K_a}},$$

These expressions are simplified by taking into account the reflections at the interfaces  $x = 0$  and  $x = L$ ; the expressions of the reflection and transmission operators are given in time domain by

$$\tilde{R}(t) = \frac{\sqrt{\alpha_\infty} - \phi}{\sqrt{\alpha_\infty} + \phi} \delta(t) - \frac{4\phi\sqrt{\alpha_\infty}(\sqrt{\alpha_\infty} - \phi)}{(\sqrt{\alpha_\infty} + \phi)^3} F\left(t, \frac{2L}{c}\right), \tag{32}$$

$$\tilde{T}(t) = \frac{4\phi\sqrt{\alpha_\infty}}{(\phi + \sqrt{\alpha_\infty})^2} F\left(t + \frac{L}{c}, \frac{L}{c}\right). \tag{33}$$

where  $\delta(t)$  is the Dirac function and  $F$  is the Green function of the medium given by Eq. (27). In the next sections, we will use the reflected and transmitted waves for solving the inverse problem in order to characterize the porous materials.

### 3.1. Ultrasonic measurement of porosity, tortuosity, and viscous and thermal characteristic lengths via transmitted waves

The experimental setup consists of two transducers broadband Ultran NCT202 with a central frequency of 190 kHz in air and a bandwidth of 6 dB extending from 150 to 230 kHz [19]. A pulser/receiver 5058PR Panametrics sends pulses of 400 V. The high-frequency noise is avoided by filtering the received signals above 1 MHz. Electronic interference is eliminated by 1000 acquisition averages. The experimental setup is shown in **Figure 3**. The inverse problem is to find the parameters  $\alpha_\infty$ ,  $\phi$ ,  $\Lambda$ , and  $\Lambda'$  which minimize numerically the discrepancy function  $U(\alpha_\infty, \phi, \Lambda, \Lambda') = \sum_{i=1}^{i=N} \left( p_{exp}^t(x, t_i) - p^t(x, t_i) \right)^2$ , wherein  $p_{exp}^t(x, t_i)_{i=1,2,\dots,n}$  is the discrete set of values of the experimental transmitted signal and  $p^t(x, t_i)_{i=1,2,\dots,n}$  is the discrete set of values of the simulated transmitted signal predicted from Eq. (33). The least squares method is used for solving the inverse problem using the simplex search method (Nelder-Mead) [20] which does not require numerical or analytic gradients.

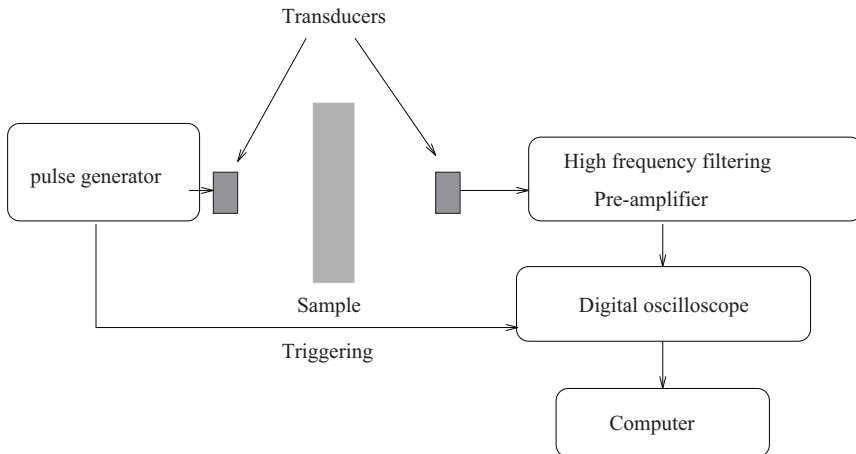


**Figure 3.** Experimental setup of the ultrasonic measurements.

Consider a sample of plastic foam M1, of thicknesses  $0.8 \pm 0.01$  cm. Sample M1 was characterized using classic methods [21–31] and gave the following physical parameters  $\phi = 0.85 \pm 0.05$ ,  $\alpha_\infty = 1.45 \pm 0.05$ ,  $\Lambda = (30 \pm 1) \mu m$ , and  $\Lambda' = (60 \pm 3) \mu m$ . **Figure 4** shows the experimental incident signal (dashed line) and the experimental transmitted signal (solid line). After solving the inverse problem simultaneously for the porosity  $\phi$ , tortuosity  $\alpha_\infty$ , and viscous and thermal characteristic lengths  $\Lambda$  and  $\Lambda'$ , we find the following optimized values:  $\phi = 0.87 \pm 0.01$ ,  $\alpha_\infty = 1.45 \pm 0.01$ ,  $\Lambda = (32.6 \pm 0.5) \mu m$ , and  $\Lambda' = (60 \pm 0.5) \mu m$ . The values of the inverted parameters are close to those obtained by conventional methods [21–31]. We present in **Figures 5** and **6** the variation of the minimization function  $U$  with the porosity, tortuosity, viscous characteristic length, and the ratio between  $\Lambda'$  and  $\Lambda$ . In **Figure 7**, we show a comparison between an experimental transmitted signal and simulated transmitted signal for the optimized values of  $\phi$ ,  $\alpha_\infty$ ,  $\Lambda$ , and  $\Lambda'$ . The difference between the two curves is small, which leads us to conclude that the optimized values of the physical parameters are correct.

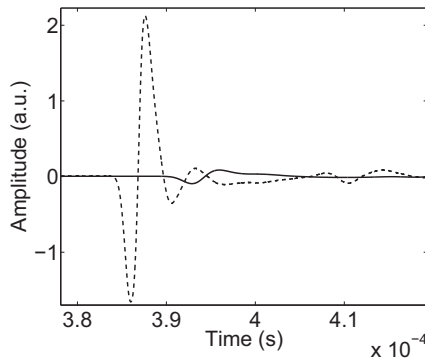


**Figure 4.** Experimental incident signal (solid line) and experimental transmitted signal (dashed line).

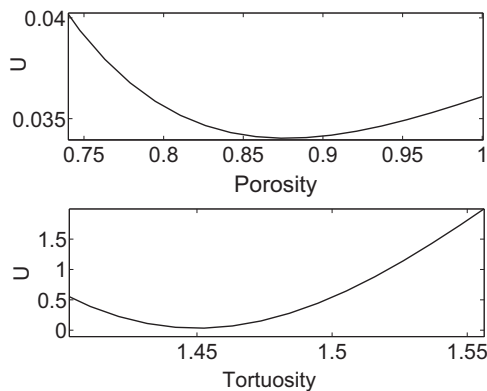


**Figure 5.** Variation of the minimization function  $U$  with porosity and tortuosity.

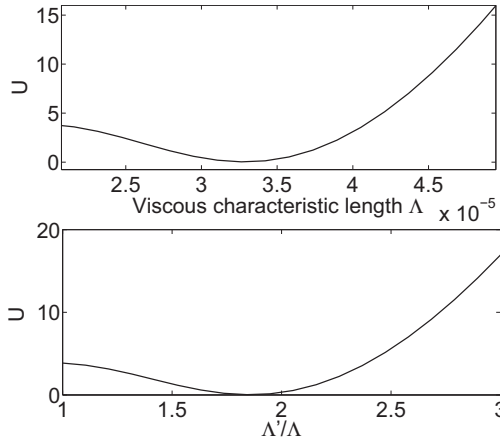


Figure 6. Variation of the cost function  $U$  with the viscous characteristic length  $\Lambda$  and the ratio  $\Lambda'/\Lambda$ .

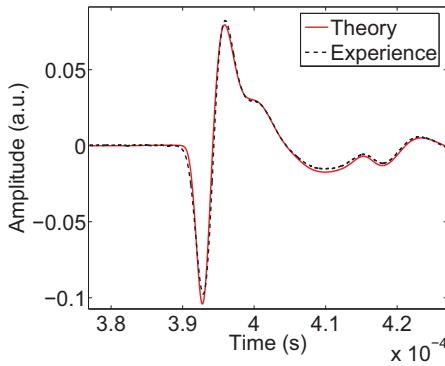


Figure 7. Comparison between the experimental transmitted signal (black dashed line) and the simulated transmitted signals (black line) using the reconstructed values of  $\varphi$ ,  $\alpha_{\infty}$ ,  $\Lambda$ , and  $\Lambda'$ .

### 3.2. Measuring flow resistivity of porous material via acoustic reflected waves at low-frequency domain

In the low-frequency domain, the viscous forces are important everywhere in all the fluid saturating the porous material. The thermal exchanges between fluid and structure are favored by the slowness of the cycle of expansion and compression in the material. The temperature of the frame is practically unchanged by the passage of the sound wave because of the high value of its specific heat: the frame acts as a thermostat; the isothermal compressibility is directly applicable. In this domain, the viscous skin thickness  $\delta = (2\eta/\omega\rho_0)^{1/2}$  is much larger than the radius of the pores  $r$

$$\frac{\delta}{r} \gg 1. \tag{34}$$

We consider the low-frequency approximations of the response factor  $\alpha(\omega)$  and  $\beta(\omega)$ . When  $\omega \rightarrow 0$ , Eqs. (22) and (6), respectively, become

$$\alpha(\omega) = \frac{\sigma\phi}{i\omega\rho}, \tag{35}$$

$$\beta(\omega) = \gamma. \tag{36}$$

For a wave traveling along the direction  $ox$ , the generalized forms of the basic Eqs. (19) in the time domain are now

$$\sigma\phi V = -\frac{\partial p}{\partial x} \quad \text{and} \quad \frac{\gamma}{K_a} \frac{\partial p}{\partial t} = -\frac{\partial v}{\partial x} \tag{37}$$

where the Euler equation is reduced to Darcy's law which defines the static flow resistivity  $\sigma = \eta/k_0$ . The wave equation in time domain is given by

$$\frac{\partial^2 p}{\partial x^2} + \left(\frac{\sigma\phi\gamma}{K_a}\right) \frac{\partial p}{\partial t} = 0 \tag{38}$$

The fields which are varying in time, the pressure, the acoustic velocity, etc. follow a diffusion equation with the diffusion constant:

$$D = \frac{K_a}{\sigma\phi\gamma}. \tag{39}$$

The diffusion constant  $D$  is connected to Darcy's constant  $k_0$  (called also the viscous permeability) by the relation

$$D = \frac{K_a k_0}{\eta\phi\gamma}, \tag{40}$$

where  $\eta$  is the fluid viscosity.

The expression of the reflection coefficient  $R(z)$  in Laplace domain (put  $z = j\omega$  for obtaining the frequency domain of  $R(\omega)$ ), is given by [32]

$$R(z) = \frac{(1 - B^2 z) \sinh(L\sqrt{Dz})}{2B\sqrt{z} \cosh(L\sqrt{Dz}) + (1 + B^2 z) \sinh(L\sqrt{Dz})}, \tag{41}$$

The development of these expressions in exponential series leads to the reflection coefficient:

$$R(z) = \frac{1 - B\sqrt{z}}{1 + B\sqrt{z}} \sum_{n \geq 0} \left(\frac{1 - B\sqrt{z}}{1 + B\sqrt{z}}\right)^{2n} \left(\exp(-2nL\sqrt{Dz}) - \exp(-2(n+1)L\sqrt{Dz})\right). \tag{42}$$

The multiple reflections in the material are taken into account in these expressions. As the attenuation is high in the porous materials, the multiple reflection effects are negligible. Let us consider the reflections at the interfaces  $x = 0$  and  $x = L$ :

$$\begin{aligned}
 R(z) &= \frac{1 - B\sqrt{z}}{1 + B\sqrt{z}} \left( 1 - \frac{4B\sqrt{z}}{(1 + B\sqrt{z})^2} \exp(-2L\sqrt{Dz}) \right) \\
 &= \frac{1 - B\sqrt{z}}{1 + B\sqrt{z}} - \frac{4B\sqrt{z}(1 - B\sqrt{z})}{(1 + B\sqrt{z})^3} \exp(-2L\sqrt{Dz})
 \end{aligned} \tag{43}$$

The reflection scattering operator is calculated by taking the inverse Laplace transform of the reflection coefficient.

We infer [32] that

$$\begin{aligned}
 \mathcal{L}^{-1} \left[ \frac{1 - B\sqrt{z}}{(1 + B\sqrt{z})} \right] &= \mathcal{L}^{-1} \left[ -1 + \frac{2}{B} \frac{1}{\sqrt{z} + 1/B} \right] \\
 &= -\delta(t) + \frac{2}{B\sqrt{\pi t}} - \frac{2}{B^2} \exp(t/B^2) \operatorname{erf}(\sqrt{t}/B),
 \end{aligned} \tag{44}$$

where erf is the error function. By putting

$$g(z) = \frac{Bz - 1}{(1 + Bz)^3} = \frac{1}{B^2} \frac{z - 1/B}{(1/B + z)^3},$$

we obtain

$$\mathcal{L}^{-1}[g(z)] = f(t) = \frac{1}{B^2} \mathcal{L}^{-1} \left[ \frac{z - 1/B}{(1/B + z)^3} \right] = \frac{1}{B^2} (t - t^2/B) \exp(-t/B).$$

Using the relation

$$\begin{aligned}
 \mathcal{L}^{-1} \left[ \sqrt{z} g(\sqrt{z}) \right] &= \frac{1}{2\sqrt{\pi}} \frac{1}{t^{3/2}} \int_0^\infty \exp\left(-\frac{u^2}{4t}\right) \left(\frac{u^2}{2t} - 1\right) f(u) du \\
 &= \frac{1}{2\sqrt{\pi B^2}} \frac{1}{t^{3/2}} \int_0^\infty \exp\left(-\frac{u^2}{4t}\right) \left(\frac{u^2}{2t} - 1\right) \left(u - \frac{u^2}{B}\right) \exp\left(-\frac{u}{B}\right) du,
 \end{aligned}$$

which with the variable change  $u/B = y$ , yields

$$\begin{aligned}
 \mathcal{L}^{-1} \left[ \frac{4B\sqrt{z}(B\sqrt{z} - 1)}{(1 + B\sqrt{z})^3} \right] &= \frac{2}{B\sqrt{\pi}} \frac{1}{t^{3/2}} \int_0^\infty \exp\left(-\frac{u^2}{4t}\right) \left(\frac{u^2}{2t} - 1\right) \left(u - \frac{u^2}{B}\right) \exp\left(-\frac{u}{B}\right) du, \\
 &= \frac{2B}{\sqrt{\pi}} \frac{1}{t^{3/2}} \int_0^\infty \exp\left(-\frac{B^2 y^2}{4t}\right) \left(\frac{y^2 B^2}{2t} - 1\right) (y - y^2) \exp(-y) dy. \\
 &= k(t)
 \end{aligned}$$

The reflection scattering operator is then given by

$$\tilde{R}(t) = (f(t) + k(t)) * g(t) \tag{45}$$

### 3.2.1. Acoustic parameter sensitivity

Consider a sample of porous material having a physical parameters that correspond to quite common acoustic materials, as follows: thickness  $L = 4$  cm, porosity  $\phi = 0.9$ , flow resistivity  $\sigma = 30000 \text{ N m}^{-4}\text{s}$ , and radius of the pore  $r = 70 \mu\text{m}$ . Let us study the sensitivity of the main parameters using numerical simulations of waves reflected by a porous material. Fifty percent variation is applied to the physical parameters (flow resistivity  $\sigma$  and porosity  $\phi$ ).

To obtain the simulated reflected waves, we use the incident signal given in **Figure 8** (dashed line). The result (reflected wave) is the wave given in the same figure (**Figure 8**) in solid line. The spectra of the two waves (incident and reflected) are given in **Figure 9**. From **Figure 8**, we can see that there is just an attenuation of the reflected wave without dispersion, since the two waves have the same spectral bandwidth (**Figure 9**). **Figure 8** shows the results obtained after reducing flow resistivity by 50% of its initial value. The wave in dashed line corresponds to the simulated reflected signal for  $\sigma = 30000 \text{ N m}^{-4}\text{s}$  and the second one (solid line) to  $\sigma = 15000 \text{ N m}^{-4}\text{s}$ . The values of the porosity  $\phi = 0.9$  and thickness  $L = 4$  cm have been kept constant. When the flow resistivity is reduced, the amplitude of reflected wave decreases by 30% of its initial value. Physically, by reducing the flow resistivity, the medium is less resistive, since the viscous effects become less important in the porous material, and thus the amplitude of the reflected wave decreases. No change is observed in the reflected wave when reducing the porosity by 50% of its initial value. We can conclude that the porosity has no significant sensitivity in reflected mode.

For the propagation of transient signals at low frequency, a guide (pipe) [32], having a diameter of 5 cm and of length 50 m, is chosen. The pipe can be rolled without perturbations on experimental signals (the cutoff frequency of the tube  $f_c \sim 4 \text{ kHz}$ ). The same microphone (Brüel & Kjær, 4190) is used for measuring the incident and reflected signals. Burst is

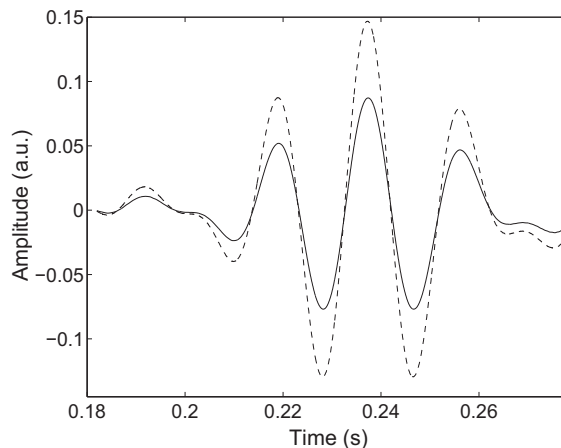


**Figure 8.** Incident signal (dashed line) and simulated reflected signal (solid line).

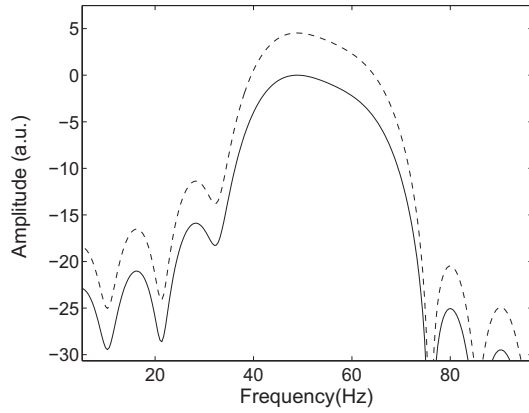


Figure 9. Spectrum of incident signal (dashed line) and spectrum of reflected signal (solid line).

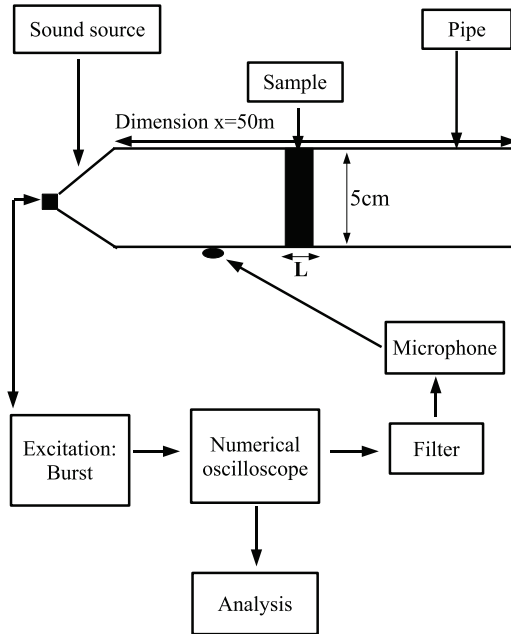


Figure 10. Experimental setup of acoustic measurements.

provided by synthesized function generator Stanford Research Systems model DS345-30 MHz. A sound source driver unit “Brand” constituted by loudspeaker Realistic 40-9000 is used. The incident signal is measured by putting a total reflector in the same position than the porous sample. The experimental setup is shown in **Figure 10**. Consider a cylindrical sample of plastic foam M1 of flow resistivity value  $\sigma = 40000 \pm 6000 \text{ Nm}^{-4}\text{s}$ . This value is

obtained using the method of Bies and Hansen [33]. The sample M1 has a diameter of 5 cm and a thickness of 3 cm. **Figure 11** shows the experimental incident wave (solid line) generated by the loudspeaker in the frequency bandwidth (35–75) Hz, and the experimental reflected signal (dashed line), with their spectra. There is no dispersion, since the two signals have practically the same bandwidth. The minimization of the function  $U$  gives the solution if the inverse problem:

$$U(\sigma) = \sum_{i=1}^{i=N} \left( p_{exp}^r(x, t_i) - p^r(x, t_i) \right)^2, \quad (46)$$

where  $p_{exp}^r(x, t_i)_{i=1,2,\dots,N}$  and  $p^r(x, t_i)_{i=1,2,\dots,N}$  represent the discrete set of values of the experimental reflected signal and of the simulated reflected signal, respectively. The optimized

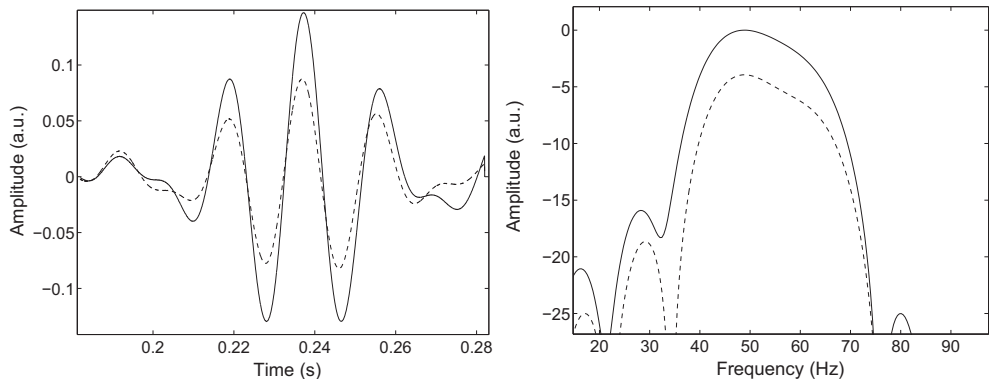


**Figure 11.** Experimental incident signal (solid line) and experimental reflected signal (dashed line), and their spectra, respectively.

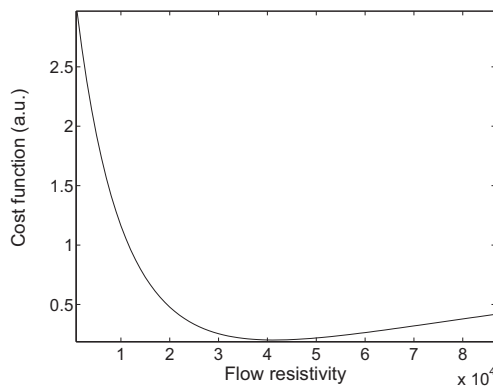


**Figure 12.** Variation of the minimization function  $U$  with flow resistivity  $\sigma$ .

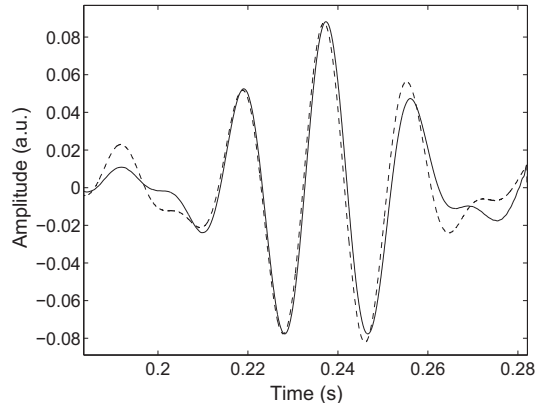


**Figure 13.** Comparison between experimental reflected signal (dashed line) and simulated reflected signal (solid line) for the sample M1.

value of  $\sigma = 40500 \pm 2000 \text{ Nm}^{-4}\text{s}$  is obtained by solving the inverse problem. The variation of the minimization function  $U$  with the flow resistivity  $\sigma$  is given in **Figure 12**. A comparison between experiment and theory is given in **Figure 13**. The difference between theory and experiment is slight, which leads us to conclude that the optimized value of the flow resistivity is good.

This alternative acoustic method has the advantage of being simple and effective since it requires the use of only one microphone and therefore no calibration problem. In addition, this approach is different from conventional methods (Bies and Hansen [33]) that involve the use of fluid flow measurement techniques and pressure differences. The mathematical analysis of the reflected wave at low frequency is quite simple, because this wave is not propagative in the medium but simply diffusive (having the same frequency band with the incident signal). The wave reflected by the resistive materials has the advantage of being easily detectable experimentally compared to the transmitted wave.

## 4. Conclusion

Acoustic propagation in porous media involves a large number of physical parameters when the structure is elastic. This number is reduced when the structure is rigid, because the mechanical part does not intervene and thus remains only the acoustic part. The study of high and low frequencies separately solves the inverse problem and characterizes the porous materials in the domain of influence of the physical parameters. The proposed methods are simple and effective and allow an acoustic characterization of porous materials using transmitted or reflected experimental waves.

## Author details

Zine El Abiddine Fellah<sup>1\*</sup>, Mohamed Fellah<sup>2</sup>, Claude Depollier<sup>3</sup>, Erick Ogam<sup>1</sup> and Farid G. Mitri<sup>4</sup>

\*Address all correspondence to: [fellah@lma.cnrs-mrs.fr](mailto:fellah@lma.cnrs-mrs.fr)

1 LMA, CNRS, UPR 7051, Aix-Marseille Univ, Centrale Marseille, Marseille, France

2 Laboratoire de Physique Théorique, Faculté de Physique, USTHB, Bab-Ezzouar, Algeria

3 LUNAM Université du Maine, UMR CNRS 6613 Laboratoire d'Acoustique de l'Université du Maine UFR STS, Le Mans, France

4 Chevron, Area 52 - ETC, Santa Fe, New Mexico, United States

## References

- [1] Biot MA. The theory of propagation of elastic waves in fluid-saturated porous solid. I. Low frequency range. *The Journal of the Acoustical Society of America*. 1956;**28**:168
- [2] Biot MA. The theory of propagation of elastic waves in fluid-saturated porous solid. I. Higher frequency range. *The Journal of the Acoustical Society of America*. 1956;**28**:179
- [3] Johnson DL, Koplik J, Dashen R. Theory of dynamic permeability and tortuosity in fluid-saturated porous media. *Journal of Fluid Mechanics*. 1987;**176**:379-402
- [4] Szabo TL. Time domain wave equations for lossy media obeying a frequency power law. *The Journal of the Acoustical Society of America*. 1994;**96**:491
- [5] Szabo TL. Causal theories and data for acoustic attenuation obeying a frequency power law. *Journal of the Acoustical Society of America*. 1995;**97**:14
- [6] Norton V, Novarini JC. Including dispersion and attenuation directly in time domain for wave propagation in isotropic media. *The Journal of the Acoustical Society of America*. 2003;**113**:3024
- [7] Chen W, Holm S. Modified Szabo's wave equation models for lossy media obeying frequency power law. *The Journal of the Acoustical Society of America*. 2003;**113**:3024
- [8] Fellah ZEA, Depollier C. Transient acoustic wave propagation in rigid porous media: A time domain approach. *The Journal of the Acoustical Society of America*. 2000;**107**(2): 683-688
- [9] Fellah ZEA, Fellah M, Lauriks W, Depollier C, Angel Y, Chapelon JY. Solution in time domain of ultrasonic propagation equation in porous material. *Wave Motion*. 2003;**38**:151-163

- [10] Fellah ZEA, Depollier C, Fellah M. Direct and inverse scattering problem in porous material having a rigid frame by fractional calculus based method. *Journal of Sound and Vibration*. 2001;**244**(2):359-366
- [11] Allard JF. *Propagation of Sound in Porous Media : Modeling Sound Absorbing Materials*. London: Chapman and Hall; 1993
- [12] Caputo M. Vibration of an infinite plate with a frequency dependent Q. *The Journal of the Acoustical Society of America*. 1976;**60**:634-639
- [13] Bagley RL, Torvik PJ. On the fractional calculus model of viscoelastic behavior. *Journal of Rheology*. 1983;**30**:133-155
- [14] Lafarge D, Lemarnier P, Allard JF, Tarnow V. Dynamic compressibility of air in porous structures at audible frequencies. *Journal of the Acoustical Society of America*. 1996;**102**:4
- [15] Norris AN. On the viscodynamic operator in Biot's equations of poroelasticity. *Journal of Wave-Material Interaction*. 1986;**1**:365-380
- [16] Samko SG, Kilbas AA, Marichev OI. *Fractional Integrals and Derivatives Theory and Applications*. Amsterdam: Gordon and Breach Publishers; 1993
- [17] Fellah M, Fellah ZEA, Mitri FG, Ogam E, Depollier C. Transient ultrasound propagation in porous media using biot theory and fractional calculus: Application to human cancellous bone. *The Journal of the Acoustical Society of America*. 2013;**133**(4):683-688
- [18] Allard JF, Champoux Y. New empirical equations for sound propagation in rigid frame fibrous materials. *Journal of the Acoustical Society of America*. 1992;**91**:3346-3353
- [19] Fellah ZEA, Sadouki M, Fellah M, Mitri FG, Ogam E, Depollier C. Simultaneous determination of porosity, tortuosity, viscous and thermal characteristic lengths of rigid porous materials. *Journal of Applied Physics*. 2013;**114**:204902-204905
- [20] Lagarias JC, Reeds JA, Wright MH, Wright PE. Convergence properties of the Nelder-mead simplex method in low dimensions. *SIAM Journal on Optimization*. 1998;**9**:112-147
- [21] Leclaire P, Kelders L, Lauriks W, Glorieux C, Thoen J. Determination of the viscous characteristic length in air-filled porous materials by ultrasonic attenuation measurements. *The Journal of the Acoustical Society of America*. 1996;**99**:1944
- [22] Ayrault C, Moussatov A, Castagnède B, Lafarge D. Ultrasonic characterization of plastic foams via measurements with static pressure variations. *Applied Physics Letters*. 1999;**74**:3224
- [23] Moussatov A, Ayrault C, Castagnède B. Porous material characterization ultrasonic method for estimation of tortuosity and characteristic length using a barometric chamber. *Ultrasonics*. 2001;**39**:195
- [24] Leclaire P, Kelders L, Lauriks W, Brown NR, Melon M, Castagnède B. Determination of viscous and thermal characteristic lengths of plastic foams by ultrasonic measurements in helium and air. *Journal of Applied Physics*. 1996;**80**:2009

- [25] Fellah ZEA, Depollier C, Berger S, Lauriks W, Trompette P, Chapelon JY. Determination of transport parameters in air saturated porous materials via ultrasonic reflected waves. *The Journal of the Acoustical Society of America*. 2003;**113**(5):2561-2569
- [26] Fellah ZEA, Berger S, Lauriks W, Depollier C, Chapelon JY. Inverse problem in air-saturated porous media via reflected waves. *Review of Scientific Instruments*. 2003;**74**(5):2871
- [27] Fellah ZEA, Berger S, Lauriks W, Depollier C, Aristégui C, Chapelon JY. Measuring the porosity and the tortuosity of porous materials via reflected waves at oblique incidence. *The Journal of the Acoustical Society of America*. 2003;**113**(5):2424
- [28] Fellah ZEA, Berger S, Lauriks W, Depollier C, Trompette P, Chapelon JY. Ultrasonic measuring of the porosity and tortuosity of air-saturated random packings of beads. *Journal of Applied Physics*. 2003;**93**:9352
- [29] Fellah ZEA, Mitri FG, Depollier D, Berger S, Lauriks W, Chapelon JY. Characterization of porous materials having a rigid frame via reflected waves. *Journal of Applied Physics*. 2003;**94**:7914
- [30] Fellah ZEA, Berger S, Lauriks W, Depollier C, Fellah M. Measurement of the porosity of porous materials having a rigid frame via reflected waves : A time domain analysis with fractional derivatives. *Journal of Applied Physics*. 2003;**93**:296
- [31] Fellah ZEA, Mitri FG, Fellah M, Ogam E, Depollier C. Ultrasonic characterization of porous absorbing materials: Inverse problem. *Journal of Sound and Vibration*. 2007;**302**:746-759
- [32] Sebaa N, Fellah ZEA, Fellah M, Lauriks W, Depollier C. Measuring flow resistivity of porous material via acoustic reflected waves. *Journal of Applied Physics*. 2005;**98**:084901
- [33] Bies DA, Hansen CH. Flow resistance information for acoustical design. *Applied Acoustics*. 1980;**13**:357-391

